Organic LETTERS

Letter

pubs.acs.org/OrgLett

Nonclassical 21-Homododecahedryl Cation Rearrangement Revisited

Said Jalife,[†] Sukanta Mondal,[†] Edison Osorio,[‡] José Luis Cabellos,[†] Gerardo Martínez-Guajardo,[§] María A. Fernández-Herrera,[*,†,∥] and Gabriel Merino[*,†]

[†]Departamento de Física Aplicada, Centro de Investigación y de Estudios Avanzados, 97310 Mérida, Yucatán, Mexico

[‡]Departamento de Ciencias Básicas, Fundación Universitaria Luis Amigó, SISCO, Transversal 51A #67B 90, Medellín, Colombia

[§]Unidad Académica de Ciencias Químicas, Área de Ciencias de la Salud, Universidad Autónoma de Zacatecas, Km. 6 carretera Zacatecas-Guadalajara s/n, Ejido La Escondida C. P. 98160 Zacatecas, Zacatecas, Mexico

[∥]Conacyt Research Fellow, Departamento de Física Aplicada, Centro de Investigación y de Estudios Avanzados, 97310 Mérida, Yucatán Mexico

Supporting Information

ABSTRACT: The degenerate rearrangement in the 21-homododecahedryl cation (**1**) has been studied via density functional theory computations and Born−Oppenheimer Molecular Dynamics simulations. Compound **1** can be described as a highly fluxional hyperconjugated carbocation. Complete scrambling of **1** can be achieved by the combination of two unveiled barrierless processes. The first one is a "rotation" of one of the six-membered rings via a 0.8 kcal·mol^{-1} barrier, and the second one is a slower interconvertion between two hyperconjomers via an out-of-plane methine bending ($\Delta G^{\ddagger}$ = 4.0 kcal·mol^{-1}).

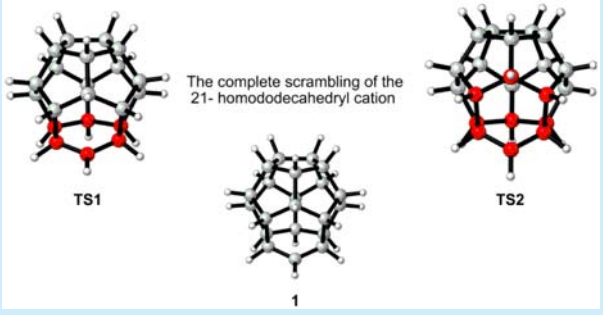

Carbocations are prone to undergo a series of rearrangements; some of them are very simple, but others involve a sequence of complex transformations.[1] In particular, degenerate rearrangements in carbocations have caught the attention of the chemistry community, mainly because after a large number of steps they conduct to the original structure. Perhaps the examples of complete carbon degeneracy par excellence are the 2-norbornyl[2−4] cation and bullvalene.[5−7] It has been observed that carbocations of the $(CH)_n^+$ series (where n is odd) are potentially degenerate carbonium ions.[1] In 1988, the group of Paquette showed degenerate rearrangements in the 21-homododecahedryl cation ($C_{21}H_{21}^+$, **1**) by ascertaining the migration of isotopic labels obtained in the solvolysis products of the monodeuterated mesylate.[8−10] This fascinating cation was described by the authors as "a most interesting electron-deficient species that has the latent potential to be the record holder for all degenerate molecules"[10] because it is capable of sustaining 2.56 × 10^{19} different arrangements!

Paquette and co-workers explored the possibility of a stereospecific process involving carbonium mesylate ion pairs, which equilibrates six of the twenty-one methine units.[9] Such a process allows the rotation of a six-membered ring (6MR) relative to a [5]peristylane fragment (Figure 1). However, this option precludes the migration of the labeled deuterium to a larger section of the cation. Thus, due to the disagreement with the deuterium labeling results it was discarded. Instead, a non-stereospecific process was proposed where more than three Wagner−Meerwein rearrangements should occur before the deuterium label finds it possible to exit the 6MR.[9]

Figure 1. Structure of the 21-homododecahedryl cation. The [5]peristylane fragment is highlighted in blue.

Herein, we revisit the rearrangement mechanism of **1**. Using density functional theory (DFT) computations and Born−Oppenheimer Molecular Dynamics (BO-MD) simulations, we identify the transition states (TSs) involved in the complete scrambling. While Paquette and co-workers discarded such a stereospecific process,[9] our computations indicate that the simultaneous operation of that with an interconversion between two hyperconjomers[11,12] (using the term defined by Schleyer et al.) explains the entire scrambling in **1**. Interestingly, both processes require very low activation energies (less than 4 kcal·mol^{-1}).

Full geometry optimizations were carried out employing the PBE0 functional[13] in conjunction with a def2-TZVP basis set using Gaussian 09.[14] Harmonic vibrational frequencies and zero-point vibrational energies (ZPVEs) were computed at the

Received: December 16, 2015
Published: February 10, 2016

DOI: 10.1021/acs.orglett.5b03558
Org. Lett. 2016, 18, 1140−1142

same level. Intrinsic reaction coordinates (IRC)[15] ensure that each TS connects with the corresponding minima. The dispersive forces were taken into account using the Grimme dispersion D3 approximation.[16] The adaptive natural density partitioning (AdNDP)[17] technique was employed to understand the nature of chemical bonding. Such methodology analyzes the first-order reduced density matrix to describe the electron density in terms of the *n*-center-two-electron (*nc*-2e) bonds. BO-MD simulations were performed at the PBE/DZVP level.[18] The simulations were started from the equilibrium geometry with the assignment of random velocities to all the atoms using a Hoover thermal bath to control the temperature. All of the BO-MD simulations were performed using the deMon-2k program.[19] A similar combination of BO-MD and high level ab initio computations has been successfully applied to elucidate the rearrangement pathways of the 2-norbornyl, 9-homocubyl, and cubyl cations.[20−23]

Compound **1** is a polyhedron composed of ten juxtaposed 5MRs and two 6MRs. Natural population analysis (NPA) charge on C21 (following the numbering scheme suggested by Paquette et al.[9]) is 0.30|e|. The formal cationic carbon C21 is depicted in red in Figure 2a, accompanied by important bond

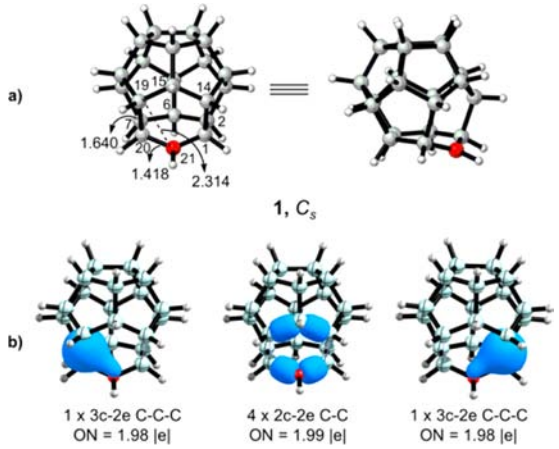

Figure 2. (a) PBE0-D3/def2-TZVP structure of **1**. Bond lengths are in angstroms. (b) AdNDP bonding pattern in **1**. ON is the occupation number.

lengths. Compound **1** adopts a C_s structure with a large degree of ring puckering as well as with significant inward distortion of the C^+ center. The short geminal C1−C21 and C20−C21 distances (1.418 Å), the long vicinal C1−C14 and C19−C20 bonds (1.640 Å), and the ring puckering facilitate the C−C hyperconjugative interactions with the "vacant" p-orbital of C21. Additionally, the computed values of C21−C1−C14 and C21−C20−C19 angles (98°) also denote hyperconjugation.[24,25] The AdNDP analysis (see Figure 2b) shows two partial 3c-2e σ-bonds around C21 with an occupation number of 1.98|e|. Therefore, despite the planar local geometry of C21, it participates in the formation of two multicenter bonds involving two long C−C interactions of 2.313 Å. Furthermore, our NBO[26] analysis indicates that the most important hyperconjugative interaction (34.2 kcal·mol^{-1}) comes precisely from the vicinal C1−C14 and C19−C20 σ-bonds to the vacant p orbital at C21 with no other important stabilizing interactions, supporting the AdNDP analysis. Thus, these results indicate that **1** is a highly hyperconjugated[24,25] carbocation with a partial nonclassical character.

During the BO-MD simulations at 600 K, **1** preserves its pattern of cage structure, but a continuous rotation of a 6MR above a [5]peristylane base is clearly perceived (see movie 1 in the Supporting Information). Remarkably, after a certain point in the simulation, a second process, which interconverts two hyperconjomers,[11] assists the complete scrambling of the twenty-one methine carbon's framework. Hence, the stereospecific process discarded by Paquette and co-workers[9] is simultaneously operating with an out-of-plane methine bending, allowing the exchange of all the CH units in **1**.

As represented in Figure 3, the "rotation" of a 6MR above a [5]peristylane moiety results in eventual equilibration of only

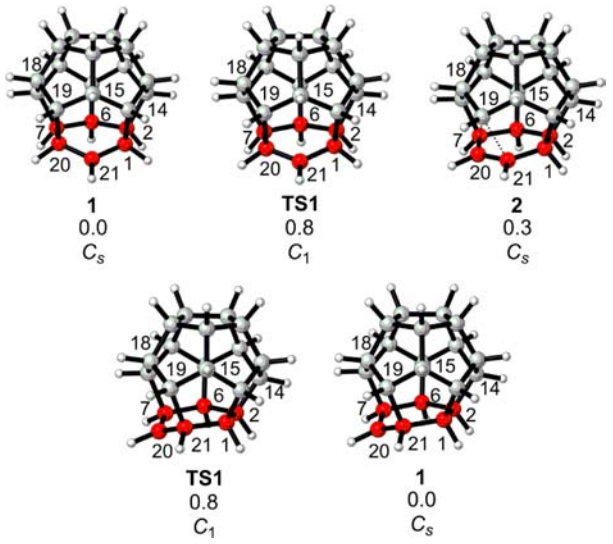

Figure 3. Stereospecific mechanism which involves the rotation of a 6MR (red) relative to a [5]peristylane fragment. Relative Gibbs free energies are given in kcal·mol^{-1}.

six methine units (C21−C1−C2−C6−C7−C20). While the carbons in the 6MR become equivalent, this stereospecific process clearly does not allow the crossover between the "low" and "high" CH fragments. The barrier for this process via **TS1**, computed at the PBE0-D3/def2-TZVP level, is very low (ΔG_{1-2} = 0.8 kcal·mol^{-1}) and involves the formation of structure **2**. Note that **1** and **2** are energetically identical, but they have some structural differences. Compound **2** is a polyhedron composed of eleven 5MRs, one 6MR, as well as a three-membered ring (3MR) formed by a well-defined 3c-2e σ-bond between the carbon atoms C21, C20, and C19 (see Figure 1, SI). Structure **2** can return to **1** via the same transition state, but the formal cationic carbon is now C20.

The second transition state (**TS2**) interconverts two hyperconjomers of **1** by an out-of-plane bending of a methine group (at C21). **TS2** has C_{2v} symmetry and resembles a typical tertiary carbocation (see Figure 4). The computed activation barrier for this process is only 4.0 kcal·mol^{-1}. The formal cationic carbon is retained at C21, but a new 6MR (composed of C21−C1−C14−C15−C19−C20 and denoted in red in Figure 3) may rotate.

In conclusion, **1** is a highly fluxional hyperconjugated carbocation that undergoes a complete scrambling only when both the 6MR "rotation" and the interconversion of hyperconjomers are simultaneously orchestrated. The electronic delocalization in **1** facilitates its dynamic behavior. While the "rotation" of 6MR allows a partial exchange with a 0.8 kcal·

DOI: 10.1021/acs.orglett.5b03558
Org. Lett. 2016, 18, 1140−1142

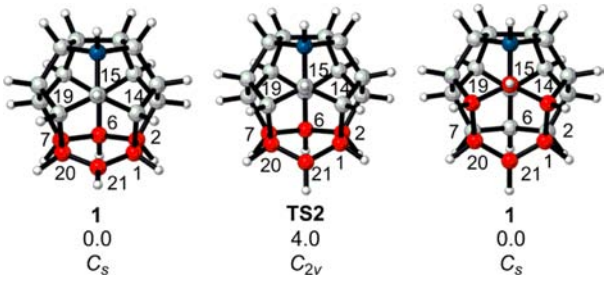

Figure 4. Degenerated rearrangement which shows the movement of the methine unit. Relative Gibbs free energies are given in kcal·mol^{-1}.

mol^{-1} barrier, the second process, which involves a classical transition state, allows the crossover between the "low" and "high" CH fragments with a barrier lower than 4 kcal·mol^{-1}. Furthermore, a bridged nonclassical stationary point (**2**) is also involved in the scrambling mechanism, and it is isoenergetic to **1**. Thus, two different types of carbocations (i.e., **1** and **2**) are involved in the degeneracy of the 21-homododecahedryl cation.

■ ASSOCIATED CONTENT

Supporting Information

The Supporting Information is available free of charge on the ACS Publications website at DOI: 10.1021/acs.orglett.5b03558.

Complete AdNDP analysis for **1** and **2** and Cartesian coordinates of all the stationary points involved in the scrambling of **1** (PDF)

BOMD simulations at 600 K for **1** (AVI)

■ AUTHOR INFORMATION

Corresponding Authors

*E-mail: mfernandez@mda.cinvestav.mx.

*E-mail: gmerino@mda.cinvestav.mx.

Notes

The authors declare no competing financial interest.

■ ACKNOWLEDGMENTS

We acknowledge Conacyt for Grant nos. CB-176863 and INFRA-252665, the postdoctoral fellowship to S.M. provided by the Red Temática de Fisicoquímica Teórica, and the Ph.D. fellowship to S.J. The CGSTIC at Cinvestav is acknowledged for the allocation of computational resources. M.A.F.-H. thanks the "For Women in Science Program" for the L'Oréal–UNESCO–Conacyt–AMC fellowship.

■ REFERENCES

(1) Leone, R. E.; Schleyer, P. v. R. *Angew. Chem., Int. Ed. Engl.* **1970**, *9*, 860.

(2) Saunders, M.; Schleyer, P. v. R.; Olah, G. A. *J. Am. Chem. Soc.* **1964**, *86*, 5680.

(3) Schleyer, P. v. R.; Watts, W. E.; Fort, R. C.; Comisarow, M. B.; Olah, G. A. *J. Am. Chem. Soc.* **1964**, *86*, 5679.

(4) Schleyer, P. v. R.; Sieber, S. *Angew. Chem., Int. Ed. Engl.* **1993**, *32*, 1606.

(5) Oth, J. F. M.; Merényi, R.; Engel, G.; Schröder, G. *Tetrahedron Lett.* **1966**, *7*, 3377.

(6) Schröder, G.; Oth, J. F. M.; Merényi, R. *Angew. Chem., Int. Ed. Engl.* **1965**, *4*, 752.

(7) Doering, W. v. E.; Roth, W. R. *Tetrahedron* **1963**, *19*, 715.

(8) Paquette, L. A. *Chem. Rev.* **1989**, *89*, 1051.

(9) Paquette, L. A.; Kobayashi, T.; Kesselmayer, M. A. *J. Am. Chem. Soc.* **1988**, *110*, 6568.

(10) Paquette, L. A.; Kobayashi, T.; Kesselmayer, M. A.; Gallucci, J. C. *J. Org. Chem.* **1989**, *54*, 2921.

(11) Rauk, A.; Sorensen, T. S.; Schleyer, P. v. R. *J. Chem. Soc., Perkin Trans. 2.* **2001**, *6*, 869.

(12) Tantillo, D. J.; Schleyer, P. v. R. *Org. Lett.* **2013**, *15*, 1725.

(13) Adamo, C.; Barone, V. *J. Chem. Phys.* **1999**, *110*, 6158.

(14) Frisch, M. J.; Trucks, G. W.; Schlegel, H. B.; Scuseria, G. E.; Robb, M. A.; Cheeseman, J. R.; Scalmani, G.; Barone, V.; Mennucci, B.; Petersson, G. A.; Nakatsuji, H.; Caricato, M.; Li, X.; Hratchian, H. P.; Izmaylov, A. F.; Bloino, J.; Zheng, G.; Sonnenberg, J. L.; Hada, M.; Ehara, M.; Toyota, K.; Fukuda, R.; Hasegawa, J.; Ishida, M.; Nakajima, T.; Honda, Y.; Kitao, O.; Nakai, H.; Vreven, T.; Montgomery, J., Jr.; Peralta, J. E.; Ogliaro, F.; Bearpark, M.; Heyd, J. J.; Brothers, E.; Kudin, K. N.; Staroverov, V. N.; Kobayashi, R.; Normand, J.; Raghavachari, K.; Rendell, A.; Burant, J. C.; Iyengar, S. S.; Tomasi, J.; Cossi, M.; Rega, N.; Millam, N. J.; Klene, M.; Knox, J. E.; Cross, J. B.; Bakken, V.; Adamo, C.; Jaramillo, J.; Gomperts, R.; Stratmann, R. E.; Yazyev, O.; Austin, A. J.; Cammi, R.; Pomelli, C.; Ochterski, J. W.; Martin, R. L.; Morokuma, K.; Zakrzewski, V. G.; Voth, G. A.; Salvador, P.; Dannenberg, J. J.; Dapprich, S.; Daniels, A. D.; Farkas, Ö.; Foresman, J. B.; Ortiz, J. V.; Cioslowski, J.; Fox, D. J. *Gaussian 09*; Gaussian: Wallingford CT, 2009.

(15) Fukui, K. *Acc. Chem. Res.* **1981**, *14*, 363.

(16) Grimme, S.; Antony, J.; Ehrlich, S.; Krieg, H. *J. Chem. Phys.* **2010**, *132*, 154104.

(17) Zubarev, D. Y.; Boldyrev, A. I. *Phys. Chem. Chem. Phys.* **2008**, *10*, 5207.

(18) Perdew, J. P.; Burke, K.; Ernzerhof, M. *Phys. Rev. Lett.* **1996**, *77*, 3865.

(19) Koster, A. M.; Geudtner, G.; Calaminici, P.; Casida, M. E.; Dominguez, V. D.; Flores-Moreno, R.; Gamboa, G. U.; Goursot, A.; Heine, T.; Ipatov, A.; Janetzko, F.; Campo, J. M. d.; Reveles, J. U.; Vela, A.; Zuniga-Gutierrez, B.; Salahub, D. R. *deMon-2k*; The deMon Developers Cinvestav: Mexico City, 2011.

(20) Jalife, S.; Martínez-Guajardo, G.; Zavala-Oseguera, C.; Schleyer, P. v. R.; Merino, G. *Eur. J. Org. Chem.* **2014**, *35*, 7955.

(21) Jalife, S.; Wu, J. I.; Martínez-Guajardo, G.; Schleyer, P. v. R.; Fernández-Herrera, M. A.; Merino, G. *Chem. Commun.* **2015**, *51*, 5391.

(22) Jalife, S.; Mondal, S.; Cabellos, J. L.; Martínez-Guajardo, G.; Fernández-Herrera, M. A.; Merino, G. *Chem. Commun.* **2016**, DOI: 10.1039/C5CC10568D.

(23) In order to explore complex isomerizations, other methodologies have been successfully employed. See: Lobb, K. *Eur. J. Org. Chem.* **2015**, 5370.

(24) Alabugin, I. V.; Gilmore, K. M.; Peterson, P. W. *Wiley Interdiscip. Rev. Comput. Mol. Sci.* **2011**, *1*, 109.

(25) Wu, J. I.; Schleyer, P. v. R. *Pure Appl. Chem.* **2013**, *85*, 921.

(26) In the NBO formalism, the magnitude of hyperconjugative stabilization between a donor–acceptor localized orbital pair (i,j) is proportional to the square of their off-diagonal Fock matrix elements (F_{ij}). The F_{ij} term corresponds roughly to the degree of orbital "mixing" and can be related to the overlap of the preorthogonal donor–acceptor orbital pair via a Mulliken-type approximation.

DOI: 10.1021/acs.orglett.5b03558
Org. Lett. 2016, 18, 1140–1142